Modification of Cyanate Ester Resin by Hydroxyl-Terminated Liquid Butadiene-Acrylonitrile Rubber and Free Volume Properties of Their Composites

Zeng Minfeng,[1] Sun Xudong,[1] Yao Xiandong,[1] Wang Yun,[1] Zhang Mingzhu,[1] Wang Baoyi,[2] Qi Chenze[1]

[1]*Institute of Applied Chemistry, College of Chemistry and Chemical Engineering, Shaoxing University, Shaoxing 312000, People's Republic of China*
[2]*Institute of High Energy Physics, The Chinese Academy of Science, Beijing 100049, People's Republic of China*

Received 19 November 2008; accepted 14 July 2009
DOI 10.1002/app.31135
Published online 27 August 2009 in Wiley InterScience (www.interscience.wiley.com).

ABSTRACT: The toughness of cyanate ester resin (CE) matrix is improved significantly with addition of hydroxyl-terminated liquid butadiene-acrylonitrile rubber (HTBN). The impact strength increased from 4.4 KJ/m^2 (pure CE) to 13.3 KJ/m^2 (CE/HTBN, HTBN 10 wt %). The curing behavior of the system is studied by differential scanning calorimetric and Fourier transform infrared spectroscope. The results showed that hydroxyl groups on the HTBN chains have slight activation effect to CE curing reaction at the beginning of the cure process. The toughening mechanism is mainly caused by the flexibilizing effects of the homogeneously dispersed HTBN molecules in the CE matrix. The toughening mechanism was demonstrated from the aspect of free volume using positron annihilation lifetime spectroscopy. With addition of HTBN, the mean free-volume size of the composite is smaller than pure CE. The decrease in the mean free-volume size of the system is mainly related to the partition effects of the finely dispersed HTBN molecules to the free-volume holes of CE matrix. A dramatic increase in the interfacial area occurs in this highly miscible system. Good interfacial adhesion is also reflected from the higher I_2 of the composite. Therefore, more positrons annihilation in their free state occurs in the composites containing HTBN than pure CE. J Appl Polym Sci 115: 338–345, 2010

Key words: phase behavior; structure-property relations; toughness

INTRODUCTION

Cyanate ester (CE) resin is one of the most important kinds of thermosetting resins and has received more and more attention for its superior mechanical properties, low water absorptivity, low outgassing in curing, high environment resistance, and excellent dielectric properties. It has been widely used as adhesives and matrixes for composites. For example, it is often applied in encapsulation of electronic devices, high-temperature adhesives, and structural aerospace materials. However, like most other thermosetting resins, it has the drawback of brittleness. A number of studies have been carried out to improve the toughness of cyanate resins, such as the preparation of flexibilized cyanate resins, the incorporation of monocyanates, the utilization of rubber-toughening technologies, the use of organoclay toughening, and the preparation of semi-interpenetrating networks have been proven useful.[1,2] Among them, using reactive elastomers such as liquid nitrile rubber was proven to be one of the most successful techniques.[3–12] The great majority of the studies involve CE's chemical modification with a reactive rubber, particularly carboxyl-terminated butadiene-acrylonitrile rubber (CTBN) rather than that of the same rubber backbone but amine-terminated or epoxy-terminated. The main reason is often attributed to higher reactivity of the carboxylic acid terminated groups. Few studies have focused on another type of nitrile rubber, i.e. hydroxyl-terminated butadiene-acrylonitrile rubber (HTBN) affects on the toughening effect to CE matrix. In fact, in epoxy resin toughening systems, HTBN has near toughening effects with CTBN.[13,14] An additional benefit is that HTBN is cheaper in price. Enlightened from this, HTBN may be a good candidate modifier to CE matrix like other reactive nitrile rubbers.

Positron annihilation lifetime spectroscopy (PALS) has been used as a unique technique to probe nano-

Additional Supporting Information may be found in the online version of this article

Correspondence to: Z. Minfeng (zengmf@zscas.edu.cn) or Q. Chenze (qichenze@zscas.edu.cn).

Contract grant sponsor: National Natural Science Foundation of China; contract grant number: 10875079.

Contract grant sponsor: Natural Science Foundation of Zhejiang Province, China; contract grant number: Y4080448.

scale voids and the free volume properties of polymers for many years.[15–18] The positrons emitted are thermalized by inelastic collisions with the surrounding media. The thermalization process will cause ionization of the media with production of secondary electrons, which can form a bound positron-electron pair, Positronium (Ps). There are two kinds of Ps atoms. The para-positronium (*p*-Ps), in which the spins of the positron and electron are antiparallel, has a lifetime of 0.125 ns by self-annihilation in vacuum, whereas the ortho-positronium (*o*-Ps), in which the spins of the positron and electron are parallel, has a longer lifetime of 142 ns in vacuum. In molecular solids three annihilation processes are possible: free positron, *o*-Ps, and *p*-Ps annihilation. Free positrons have a lifetime of about 0.4 ns through interaction with the outer electrons of molecules with which they collide. *o*-Ps atoms are preferentially localized in atom-scale holes, and their lifetime is shortened to about 1−5 ns by a spin exchange or pick-off annihilation with other electrons from surrounding molecules. The *o*-Ps lifetime τ_3 directly correlates with the size of free volume holes, and its intensity I_3 contains information about the free volume concentration. The average radius (R) of free volume holes on a quantum mechanical model developed by Tao[19] was proposed as follow equation:

$$\frac{1}{\tau_3} = 2\left\{1 - \frac{R}{R+\Delta R} + \frac{1}{2\pi}\sin\left(\frac{2\pi R}{R+\Delta R}\right)\right\} \qquad (1)$$

where R is the radius of the free volume hole, ΔR (=0.1656 nm) is derived from fitting the observed *o*-Ps lifetimes in molecular solids with known hole sizes.[20] A study on the behavior of free volume in the two-component blends will help us to understand the interaction between the different macromolecular chains, the relationship between the microstructure, and the properties of blends. Our formal works[13,21,22] has shown that PALS is an effective tool to probe the atomic-scale microstructure of thermosetting resin/liquid rubber composites.

The effects of the blend composition on the cure behavior, phase separation and the properties of CE/HTBN composites have been studied in the current work. Meanwhile, the free volume properties of CE/HTBN composites have been determined with PALS. The purpose of this study is to: 1) evaluate the toughening effects of the HTBN on CE matrix, 2) discuss the toughening mechanism from the aspect of free-volume.

EXPERIMENTS

Materials

A phenolic-based CE monomers (melting point: 76°C) was supplied by Jinan Special Structure Institute of China Aero-Industry (Jinan, China). The HTBN was provided by Lanzhou Chemical Industry Compony (Lanzhou, China). The molecular weight of HTBN was between 3000—5000. The acrylonitrile content of the used HTBN was 22–25 wt %. The data of the molecular weight and acrylonitrile content of HTBN was provided by Lanzhou Chemical Industry Company (Lanzhou, China). Mold release agent (JR105 silicone grease) was supplied by Jinrong Grease Company (Fuyang, China).

Preparation of the composites

In this study, the blends are designated by the weight percentage of HTBN components. For example, a binary blend containing 95 g of CE and 5 g of HTBN takes the abbreviation of HTBN 5 wt %. CE monomers were placed (about 60 g) in a beaker maintained at 90°C. Selected amounts of HTBN (rubber content: 0, 3, 5, 8, 10, 15 wt %) were added to the CE resin at 90°C with stirring. After completely mixing, mixture was quickly poured into a preheated steel mold coated with right amounts of the mold release agent (just put a cover over the steel mold) (see supporting information). After degasification under vacuum (about 1000 Pa) for 30 min at 110°C, the cure procedure for the samples was as follows (at normal pressure): 130°C/ 1 h + 150°C/ 1 h + 170°C 1 h + 190°C 1 h + 210°C/ 1 h +230°C/ 1 h + 250°C/ 1 h to form the specimens. Then the samples were cooled down naturally.

Characterization of the composites

The unnotched impact strength was measured with a Charpy impact tester (XCJ-5, Chengde Testing Machine Co., China). The tests were according to the Chinese national standard methods for impact resistance of resin casting body (GB/T 2571-1995) at 23 ± 2°C. The size of the samples for impact testing is about: 80 mm × 10 mm × 5 mm. The tensile properties were measured with a universal materials testing machine (SANS Testing Machine Co., Shenzheng, China) with a crosshead speed of 2 mm/min. The tensile measurements were according to the Chinese national standard methods for tensile properties of resin casting body (GB/T 2568-1995) at 23 ± 2°C. The sample for tensile testing is dumbbell shaped and the scale distance is 50 mm. Five specimens of each group were prepared and tested.

The reactions were tracked by infrared spectrometry with Fourier transform infrared spectroscope (FTIR-Nicolet 740). The prepolymer of CE-HTBN was blended with appropriate amount of KBr to form a sheet. The sheet was scanned first by Fourier transform infrared spectroscope (FTIR) for its initial curve, and then the sheet was placed in an oven at

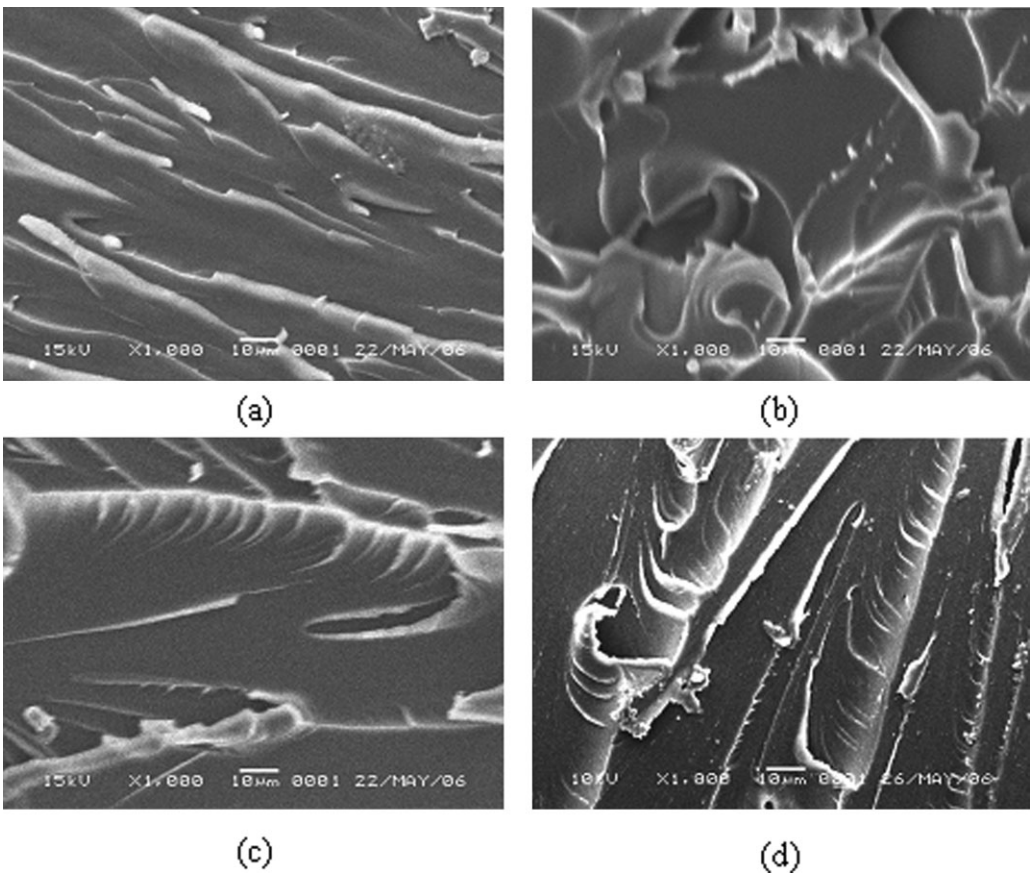

Figure 1 SEM images of the fractured surface of pure CE and CE/HTBN composites: (a) pure CE; (b) HTBN (5 wt %); (c) HTBN (8 wt %); (d) HTBN (15 wt %).

170°C for various time intervals and scanned once again by FTIR for its partial-cure curve.

Differential scanning calorimetric (DSC, PekinElmer DSC-7) measurements were made at a scan rate of 10°C/min with 4–6 mg samples in a nitrogen atmosphere.

The morphology of the composites was examined by JEM-6360 scanning electron microscopy (SEM). All the samples were coated with gold to improve SEM imaging. Before a transmission electron microscope (TEM) observation, the composite samples were cut by a ultramicrotome (Power Tome-PC, RMC Products by Boeckeler Instruments) to obtain the ultra thin film of the samples. To view phase separated rubber phase with a TEM, the ultra thin sample film was stained with Osmium tetroxide (OsO_4) and then observed with a JEM-1200EX TEM.

PALS measurement

PALS was measured with an EG&G ORTEC fast-fast lifetime spectrometer (ORTEC Co., TN) with a FWHM = 190 ps for a ^{60}Co prompt peak of 1.18 MeV and 1.33 MeV γ rays. A 6×10^5 Bq of positron source (^{22}Na) was deposited between two Kapton films (3 μm in thickness), which was sandwiched between two identical composite samples. All PALS measurements were performed at room temperature. Every spectrum contained about 10^6 counts. The resulting spectra were consistently modeled with a three-component fit with the computer program PATFIT.

RESULTS AND DISCUSSION

Phase structure and morphology

The impact fracture surface of HTBN-modified CE networks was analyzed by SEM (Fig. 1). The pure CE shows a brittle fracture surface. SEM micrographs of CE modified with HTBN do not show distinct separated particles of rubber, indicating fairly well interfacial adhesion and compatibility between the blend components. With addition of HTBN, the composites have much rougher fracture surface consisting of more and shorter crevices and all directions crack propagation. It infers that there will be a great improvement in the toughness of these blends.

Usually, during the curing reaction of thermosetting resin/ rubber systems, the rubber phase would separate and form tiny particles that dispersed in the thermosetting resin network after cure. To further confirm the phase size of the composites, the

phase structure has been observed with TEM. The unreacted double bond within the rubber phase can be stained with Osmium tetraoxide (OsO_4) and the rubber phase exhibited dark zone in the TEM photos. As shown in Figure 2, HTBN phase do not aggregate to form regular sphere. The rubber phase dispersed homogeneously with its size in nano-level (about 10 nm). The phase size is much smaller than in CE/CTBN system.[9–11,22] The phase separated rubber particle size of CE/CTBN system is about 1 μm. It refers that HTBN has much better compatibility with CE than CTBN though the terminal —COOH groups of CTBN has higher activity than terminal —OH groups of HTBN. This difference in phase behavior might be attributed to the solubility parameters of the component and the kinetics of phase separation. Referring to the literature,[23] the solubility parameter of CE is 9.41 $(cal/cm^3)^{1/2}$, HTBN[24] is 9.46 $(cal/cm^3)^{1/2}$, and CTBN[11] is 9.15$(cal/cm^3)^{1/2}$. Therefore, the better compatibility between the used HTBN with CE is proposed for their closer solubility parameters.

Curing behavior of the system

The cyclotrimerization reaction is the dominant reaction pathway during the cure of cyanate-based resins to form highly crosslinked polytriazine networks.[25,26] The reaction can be catalyzed by coordination metal catalysts and an active hydrogen initiator or thermally induced at high temperature than 190°C. Figure 3 shows the DSC results of the curing reaction of the composites. The addition of HTBN relaxed the curing reaction of CE, and the CE/HTBN system shows a broad and moderate curing peak compared to pure CE system. The onset temperature of CE curing shows a slight decrease with the addition of HTBN. This means that hydroxyl groups on the HTBN chain have slight activation effect on the CE curing reaction at the beginning of the curing process. The reason is that the hydroxyl groups on the HTBN molecule chain can supply active hydrogen to the system. Thus, the onset temperature of the cure process of the system decreases with the addition of HTBN. As seen in Figure 3, both the end temperature and the peak temperature of CE curing show a slight decrease with the addition of HTBN. But in CE/CTBN system,[22] these two temperatures show a slight increase. This is because of the better compatibility of CE/HTBN. The initial homogeneous blend is almost maintained during the cure process. The better-dispersed HTBN molecules had higher activation effects on CE. In addition, according to the DSC results, the curing exothermic heat (ΔH_{exo}) of CE/HTBN is a bit lower than CE. It suggests the addition of HTBN did not significantly change the dominant cyclotrimerization reaction of CE. The polar groups of the well-dispersed HTBN are capable to react with the polar groups of CE monomers. This will lead to a decrease to some extent in the formation of polytriazine networks. Therefore, the curing exothermic heat shows a bit decrease in CE/HTBN system.

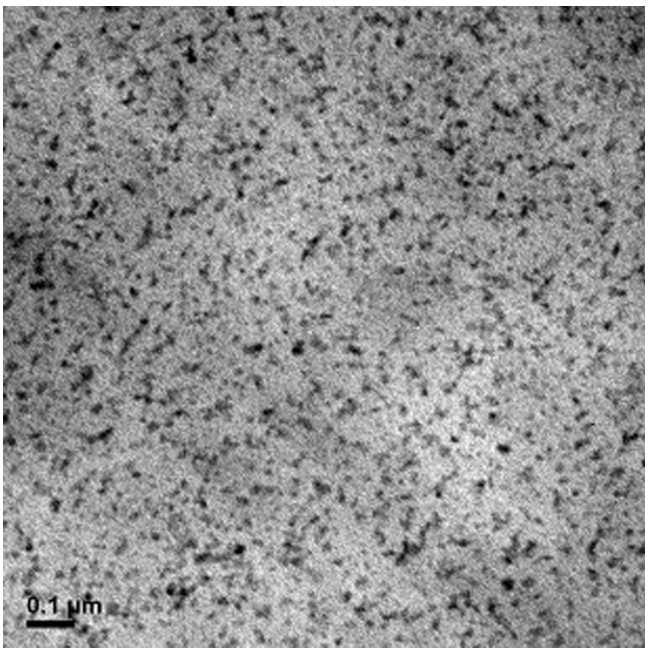

Figure 2 TEM image of CE/HTBN (HTBN 8 wt %).

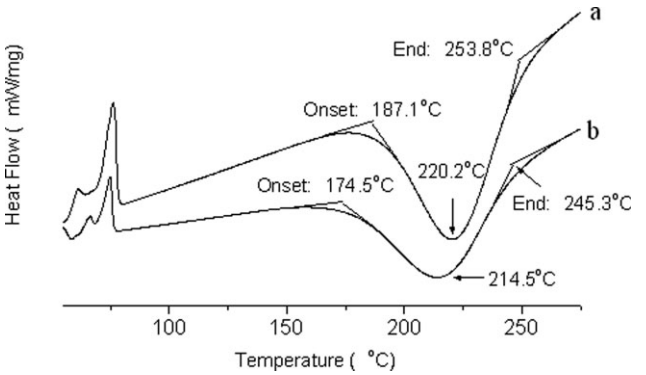

Figure 3 DSC curves of: (a) CE (ΔH_{exo} = 413.4 J/g); (b) CE/HTBN (HTBN 8 wt %) (ΔH_{exo} = 378.3 J/g).

FTIR was employed to study the influence of HTBN on the curing behavior of CE at 170°C. The reaction during cure process was tracked mainly by paying attention to the —C≡N stretching band at 2272 cm^{-1} as the cyanate group of CE resin. As shown in Figure 4, the intensity of this absorption band decreases during the cure process, and the intensity of the absorption band at 1565 cm^{-1} (—C=N stretching band of polytriazine) increased. The main reaction of the system is cyclotrimerization of the

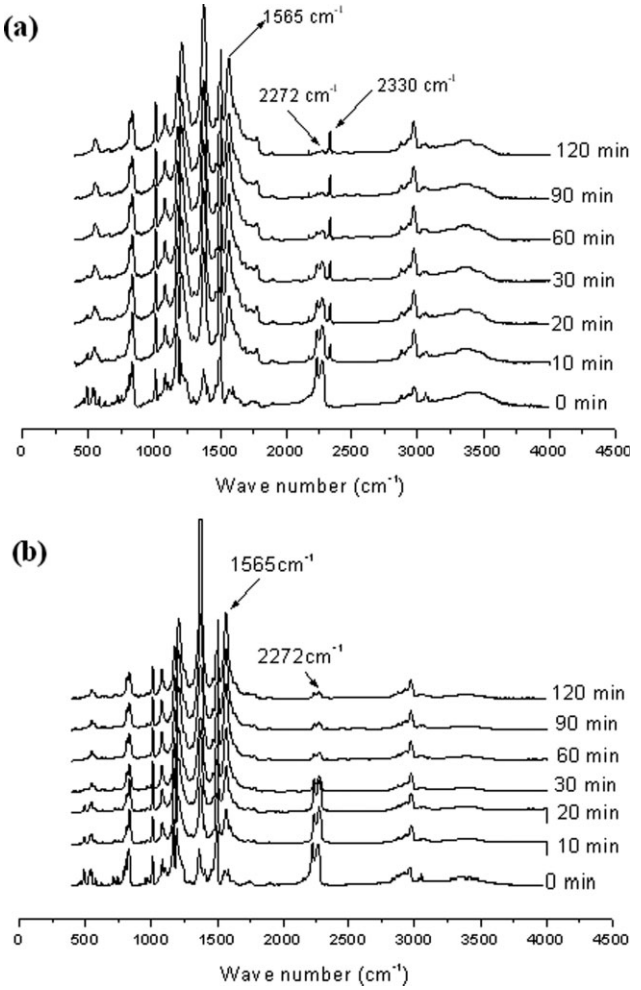

Figure 4 Curing behavior at 170°C of the composites studied by FTIR: (a) CE; (b) CE/HTBN (HTBN 8 wt %).

cyanate groups to form highly crosslinked polycyanurate network in the absence or presence of the HTBN (Scheme 1). It suggests the addition of HTBN did not significantly change the dominant cyclotrimerization reaction of CE.

As shown in Figure 4(a), a new weak absorption band at 2330 cm^{-1} is found during the cure process. Its intensity increases in the first 20 min and did not change anymore afterward. This absorption band could be attributed to the —N=C=O stretching band. At the beginning of the measurements, the reaction rate of the cyclotrimerization is relatively slow, and the cyanate groups of some CE molecules may have an isomeric change to isocyanate (Scheme 2). According to Figure 4(b), this isomeric change does not occur in the CE/HTBN system. Because of the good phase dispersion of the system during the cure process, CE molecules have great probabilities to coupling with surrounding HTBN molecules (Scheme 3). During the latter stage (after 30 min) of the isothermal curing analysis, it is found that the

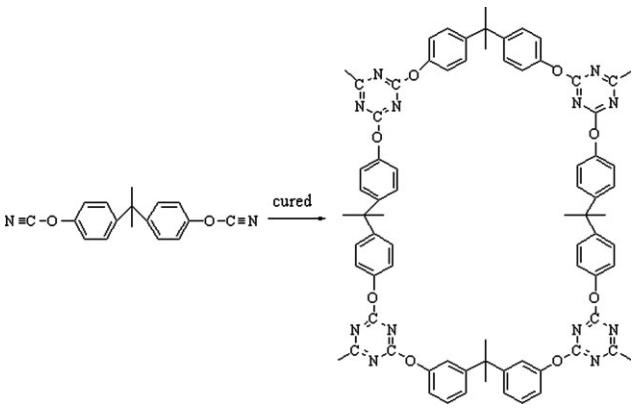

Scheme 1 Cure scheme of CE.

intensity of the absorption band at 2272 cm^{-1} decreases faster in pure CE system than CE/HTBN (HTBN 8 wt %) system. This means the gelation time of the pure CE system is a bit faster than in CE/HTBN system at 170°C. It is due to the steric effects caused by the well-dispersed HTBN. This would decrease the collision probability of CE molecules themselves.

Free volume properties of the system

The PALS spectra for all samples were analyzed with PATFIT for three or more components of lifetime. For all samples a three-component fit was much better with variances all below a value of 1.2. Usually, the shortest lifetime τ_1 is attributed to *p*-Ps annihilation. The intermediate lifetime τ_2, is from the free positron annihilation. The longest lifetime τ_3, is assigned to *o*-Ps annihilation. The HTBN content dependence of the o-Ps lifetime τ_3, its intensity I_3, and the intensity of the intermediate lifetime I_2 are shown in Figures 5 and 6. As shown in Figure 5, the o-Ps lifetime τ_3 of the composite containing HTBN is much shorter than pure CE. Its intensity I_3 also decreases as the HTBN added (0–10 wt %). The intensity of the intermediate lifetime I_2 shows an increase as the HTBN added (0–10 wt %). The case of CE containing highest HTBN content (15 wt %) has relatively higher I_3 and lower I_2 comparing with CE/HTBN in other blend mass ratio.

These changes in positron annihilation parameters can be explained as follows. Previous studies[27,28] have shown that in the case of thermosetting-based composites, chains are restricted in the rigid network structure (in which chain units connect with chemical bond) and their mobility depend much more on the properties of the network, such as chemical

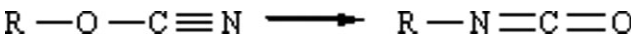

Scheme 2 Isometric change of CE.

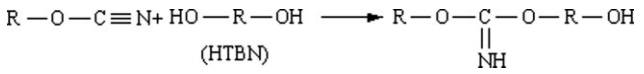

Scheme 3 Reaction between CE molecules and HTBN molecules.

structure and crosslinking density. The size and concentration of free volume holes are mainly determined by the backbone structure, which depends strongly on the conversion of cure reaction. According to eq. (1), the average radius R of the free volume holes of pure CE matrix can be calculated and its value is 0.2870 nm. The free volume radius (R) of the composites is shown in Figure 7. The changes of R are similar with the changes of *o*-Ps lifetime of the composites. All the specimens that modified with HTBN with different weight percentage have smaller free volume size than pure CE. As discussed in the curing behavior section, the cured CE/HTBN has formed a semi-IPN structure and HTBN do not have big influences on the formation of CE network, though there are some coupling products formed between CE and HTBN. The decrease in the mean free volume size of the CE/HTBN composites is not mainly caused by the changes in the network structure of the matrix but the partition effects of the homogeneously dispersed HTBN molecules. As shown in Figure 8, the well-dispersed HTBN chains can enter the free volume holes of CE matrix, leading to partition effects to the free volume hole of the CE matrix. Such partition effects would lead to a decrease in the free volume size of CE matrix. This is the main factor determining the decrease in the mean free volume size of the composite. The bigger R in the case of CE containing highest HTBN content (15 wt %) is related to the higher trend of rubber molecules aggregation during the cure process for its high rubber concentration. In addition, the contribution of *o*-Ps annihilation in the rubber phase to the lifetime component τ_3 of the composite cannot be neglected anymore when the rubber content is too high. Generally, the rubber phase is much looser than the crosslinked CE matrix because of its amorphous structure. The size of the free volume holes within the rubber phase is larger than in the CE network, resulting in an increasing effect on the mean free volume size of the composites.

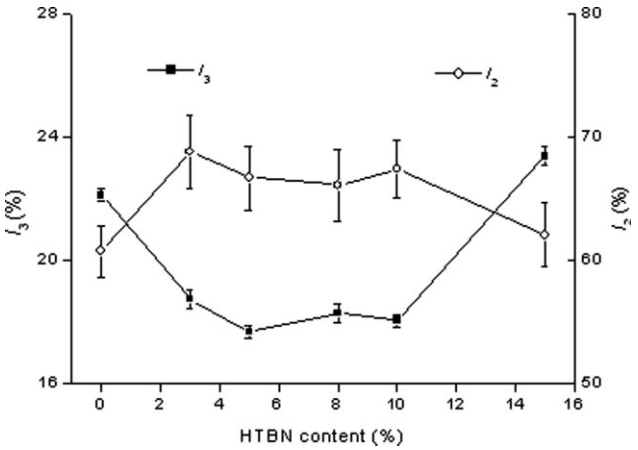

Figure 6 The intensity of the intermediate lifetime component I_2, the intensity of the *o*-Ps component I_3 of the composites with different HTBN content.

Usually, the partition effect to the free volume hole of CE matrix should lead to an increase in free volume concentration of the composites. However, as shown in Figure 6, the *o*-Ps intensity I_3 is lower than pure CE as the HTBN added (0–10 wt %). And higher intensity of the intermediate lifetime I_2 is observed. These results are related to the strong interfacial adhesion between the HTBN phase and CE matrix. For a polymer base composite filled with

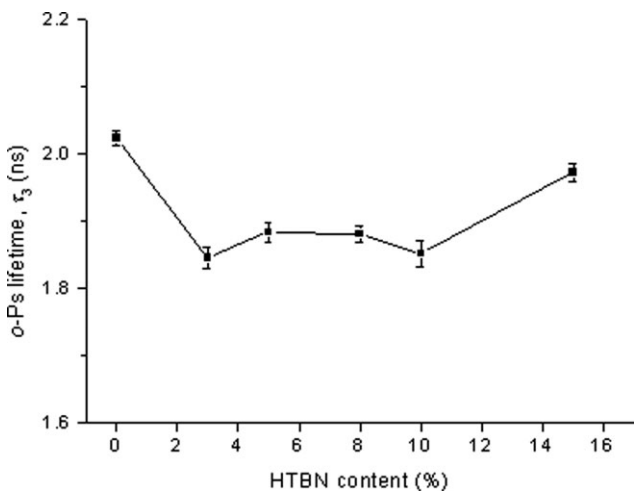

Figure 5 The *o*-Ps lifetime τ_3 of the composites with different HTBN content.

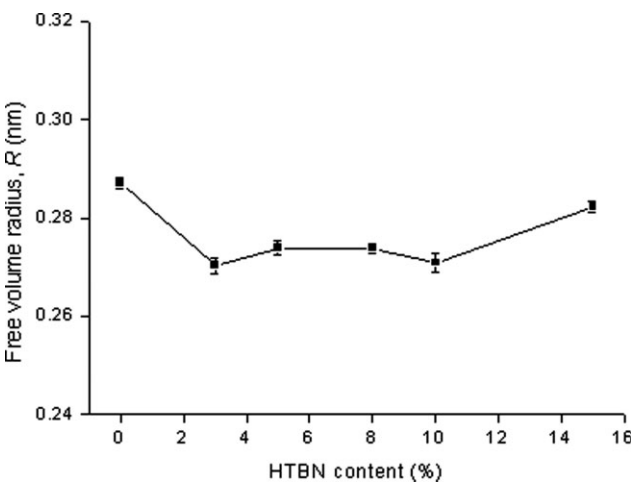

Figure 7 The calculated free volume radius R of the composites with different HTBN content.

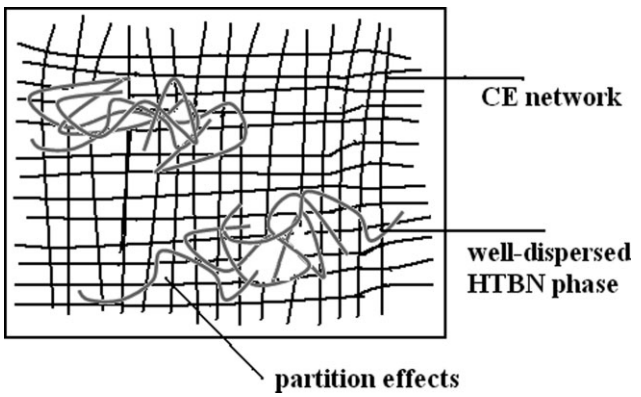

Figure 8 Fine phase morphology of the composites.

nano-particles, a correlation is that the interfacial property of the composites can be reflected in the intensity of the intermediate lifetime component I_2.[27–30] In the interfacial area, all kinds of interfacial interactions between CE matrix and HTBN phase come from the interactions of polar groups of HTBN and CE molecules. The concentrate of polar groups should be higher in interfacial zone. The polar groups are often electro-attracting for its high electro-negativity, and act as electron scavengers and positron capturers.[22,31] Therefore, the intermediate lifetime component comes not only from the free positron annihilation in the body state of the polymers but also polar groups trapping positrons in the interfacial layers for its strong interfacial adhesion. In this CE/HTBN blend system, HTBN dispersed homogeneously (in nano level) in the CE crosslinking network. A great number of interfacial layers form between the HTBN phase and CE matrix. Therefore, more positrons annihilation in their free state occurs in the composites containing HTBN than pure CE. Correspondingly, less Ps form and o-Ps annihilation decreases. In the case of CE containing highest HTBN content (15 wt %), it has obviously higher I_3 and lower I_2 comparing with CE/HTBN in other blend mass ratio. The reason can also be due to the higher trend of rubber molecules aggregation during the cure process for its high rubber concentration. Therefore, the amounts of the interfacial layers decreased and lower I_2 occurred.

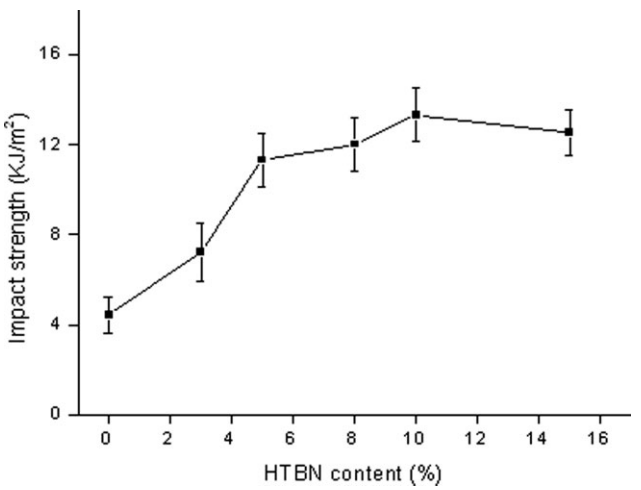

Figure 9 The impact strength of the composites with different HTBN content.

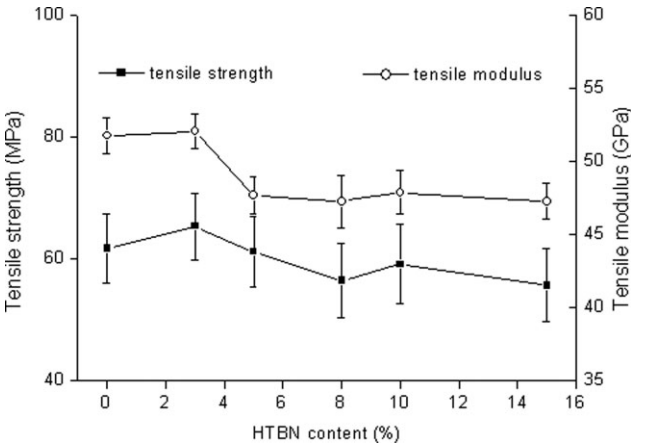

Figure 10 The tensile properties of the composites with different HTBN content.

Toughening behavior and mechanism

The impact strength of CE/HTBN composites were measured and shown in Figure 9. A significant increase in the impact strength of all the samples added with HTBN, when compared with that of pure CE is observed. The best performance (13.3 KJ/m^2) is achieved with 10% of HTBN by weight. The compatibility and interfacial adhesion of the composites can be inferred from the changes in free-volume properties of the composites.

In a thermosetting resin modified with rubber system, the impact behavior of the toughened matrix could be explained by considering both toughening and flexibilizing effects.[32,33] In such CE/HTBN system, the dominant effect is the flexibilizing effect. HTBN dispersed homogeneously in the CE matrix. A strong adhesion forms between the blend components. The CE matrix has been effectively flexibilized by the finely dispersed HTBN molecules inside the CE matrix. It is consistent with the PALS results. As seen from Figure 7, with addition of HTBN, the mean free-volume size of the composite is much smaller than pure CE. The decrease in the mean free-volume size of the system is mainly related to the partition effects of the finely dispersed HTBN molecules to the free-volume holes of CE matrix. Good interfacial adhesion is also reflected from the higher I_2 of the composite. Therefore, the toughness of the composite increases as HTBN is added. The decrease in the tensile strength and modulus (as

shown in Fig. 10) of the composites is mainly attributed to the lower modulus of the rubber component.

CONCLUSIONS

HTBN is a good candidate modifier for the improvement of the toughness of CE matrix. It is highly miscible with CE matrix. This phase behavior might be attributed to the solubility parameters of the component and the kinetics of phase separation. The toughening mechanism is mainly caused by the flexibilizing effects of the homogeneously dispersed HTBN molecules in the CE matrix. The toughening mechanism is demonstrated from the aspect of free volume using PALS. The homogeneously dispersed HTBN molecular chains can enter the free volume holes of CE matrix because the functional groups of HTBN molecular chains are capable to react with CE, leading to a partition effect to the free volume hole of the CE matrix. A dramatic increase in the interfacial area occurs in this highly miscible system. Therefore, more positrons annihilate in their free state in the composites containing HTBN than pure CE.

References

1. Mcgarry, F. J. In Polymer Toughening;Arends, C. B., Ed. Marcel Dekker: New York, 1996; p 175.
2. Huang, Y.; Hunston, D. L.; Kinloch, A. J.; Keith, R. C. Rubber Toughened Plastics, ACS Advances in Chemistry Series 233; American Chemical Society: Washington, D.C., 1993; p 1.
3. Hayes, B. S.; Seferis, J. C. Int SAMPE Symp Exhib 2001, 46, 1072.
4. Hayes, B. S.; Seferis, J. C.; Parker, G. A. Polym Eng Sci 2000, 40, 1344.
5. Borrajo, J.; Riccardi, C. C.; Williams, R. J. J.; Cao, Z. Q.; Pascault, J. P. Polymer 1995, 36, 3541.
6. Wang, J. L.; Liang, G. Z.; Zhao, W.; Lu, S. H.; Yan, H. X. Polym Eng Sci 2006, 46, 587.
7. Hillermerier, R. W.; Hayes, B. S.; Seferis, J. C. Polym Compos 1999, 20, 155.
8. Cao, Z.; Mechin, F.; Pascault, J. P. Polym Int 1994, 34, 41.
9. Feng, Y.; Fang, Z. P.; Gu, A. J. Polym Adv Technol 2004, 15, 628.
10. Feng, Y.; Fang, Z. P.; Gu, A. J. Polym Int 1994, 54, 369.
11. Shi, H. H.; Fang, Z. P.; Gu, A. J.; Tong, L. F.; Xu, Z. B. J Appl Polym Sci 2007, 106, 3098.
12. Yang, C. Z.; Gu, A. J.; Song, H. W.; Xu, Z. B.; Fang, Z. P.; Tong, L. F. J Appl Polym Sci 2007, 105, 2020.
13. Zeng, M. F.; Sun, X. D.; Xiao, H. Q.; Ji, G. Z.; Jiang, X. W.; Wang, B. Y.; Qi, C. Z. Radiat Phys Chem 2008, 77, 245.
14. Li, S. Y.; Han, X. Z.; Zhang, Q. Y. Chem J Chin U 1997, 18, 1541.
15. Ito, K.; Kobayashi, Y. Appl Phys Lett 2003, 82, 654.
16. Hu, Y. H.; Qi, C. Z.; Liu, W. M.; Wang, B. Y.; Sun, X. D.; Zheng, H. T. J Appl Polym Sci 2003, 90, 1507.
17. Jean, Y. C. Microchem J 1990, 42, 72.
18. Pethrick, R. A. Prog Polym Sci 1997, 22, 1.
19. Tao, S. J. J Chem Phys 1972, 56, 5499.
20. Nakanishi, H.; Wang, S. J.; Jean, Y. C. In Positron Annihilation Studies of Fluids;Sharma, S. C., Ed. World Science Publishing: Singapore, 1988; 292.
21. Zeng, M. F.; Sun, X. D.; Yao, X. D.; Ji, G. Z.; Chen, N.; Wang, B. Y.; Qi, C. Z. J Appl Polym Sci 2007, 106, 1347.
22. Zeng, M. F.; Sun, X. D.; Wang, Y.; Zhang, M. Z.; Shen, Y. M.; Wang, B. Y.; Qi, C. Z. Polym Adv Technol 2008, 19, 1664.
23. Srinivasan, S. A.; Mcgrath, J. E. SAMPE Q 1993, 24, 25.
24. Yang, Y. R.; Huang, Y. M.; Wang, D. N.; Liu, H. L.; Hu, C. P. Eur Polym J 2004, 40, 855.
25. Shimp, D. A.; Hudock, F. A.; Ising, S. J. Int SAMPE Symp Exhib 1988, 33, 754.
26. Gupta, A. M.; Macosko, C. W. Makromol Chem Macromol Symp 1991, 45, 105.
27. Yu, D. H.; Wang, B.; Feng, Y.; Fang, Z. P. J Appl Polym Sci 2006, 102, 1509.
28. Liu, L. M.; Fang, P. F.; Zhang, S. P.; Wang, S. J. Mater Chem Phys 2005, 92, 361.
29. Zhang, M.; Fang, P. F.; Zhang, S. P.; Wang, B.; Wang, S. J. Radiat Phys Chem 2003, 68, 565.
30. Wang, B.; Qi, N.; Gong, W.; Li, X. W.; Zhen, Y. P. Radiat Phys Chem 2007, 76, 146.
31. Qi, C. Z.; Wang, W.; Wu, Y. J.; Zhang, S. H.; Wang, H. J.; Li, H. M.; Wang, T. M.; Yan, F. Y. J Polym Sci Part B: Polym Phys 2000, 38, 435.
32. Fabio, L. B.; Thiago, P. A.; Bluma, G. S. Polymer 2003, 44, 5811.
33. Bucknall, C. B. Toughened plastics; Applied Science Publishers: London, 1977; p 188.